A Study on the Smoke Removal Characteristics of the ESP Adopting Resonant dc-dc Converter

Su-Weon Kim*, Jong-Woong Park*, Jong-Han Joung, Hyun-Ju Chung***
Jin-Young Choi* and Hee-Je Kim †

Abstract - In this study, we propose a small high voltage power supply, which uses a half-bridge ZCS resonant and Cockroft-Walton circuit as its ESP (Electrostatic Precipitator). This power supply transfers energy from the ZCS resonant inverter to the step-up transformer. The transformer secondary is then applied to the Cockroft-Walton circuit for generating high voltage as a discharging source of electrodes. It is highly efficient because its amount of switching losses are reduced by virtue of the current resonant half-bridge inverter, and also due to the small size, low parasitic capacitance in the transformer stage owing to the low number of winding turns of the step up transformer secondary combined with the Cockroft-Walton circuit. Using this power supply, experiments have been carried out as a function of the switching frequency and duty ratio in order to investigate the smoke removal characteristics. From these results, the best operational condition is obtained at the switching frequency of 9 kHz and the duty ratio of 50% in this ESP.

Keywords: Cockroft-Walton circuit, ESP (Electrostatic Precipitator), High voltage power supply, Smoke removing characteristics.

1. Introduction

Currently, there are several important environmental problems in the world. One of them is air pollution arising from combustion flue gases produced by thermal power plants, factories and motor vehicles. At the present time calcium-gypsum (De-SOx), ammonia-catalytic (De-NOx) and air filter methods are used as treatments of air pollution. Although these processes are effective and reliable, the initial and running costs are very high [1].

ESP and bag-house filters are the most common industrial scale particulate control systems. The state-of-the-art bag-house filters can capture particles well; however the pressure drop of the filter becomes unacceptably high for economical removal of very fine matter [2].

An electrostatic precipitator is an air pollution control device that removes particles from a flowing gas by way of electric forces. The electrical force acts for the most part on the particles and not the gas. Thus, the pressure drop is very low compared to other control options. ESP is used in industry (for example, steel mills, pulp/paper plants, cement kilns, and waste incineration), coal-fired electric power plants, and indoors in homes and offices [3].

† Corresponding Author: Dept. of Electrical Engineering, Pusan National University, Korea. (heeje@pusan.ac.kr)
* Dept. of Electrical Engineering, Pusan National University, Korea. (nonpahada@hanmail.net)
** Dept. of Electrical and Electronic Engineering, Changwon College, Korea. (ivan1@hanmail.net)
Received December 30 2003 ; Accepted May 6, 2004

In this study, we fabricated a small high power supply for ESP, which uses a half-bridge ZCS resonant inverter and Cockroft-Walton voltage multiplier. The electric energy from the ZCS resonant inverter was transferred to the step-up transformer and the transformer secondary was applied to a voltage multiplier for generating high voltage as a discharge source of the electrode. This combination guarantees small parasitic capacitance in the transformer stage, and rapid dynamic response. In particular, the ZCS series resonant inverter was used to decrease the losses by the tailing current generated upon turning off of the IGBT (Insulated gate bipolar transistor). As such, the ESP has many advantages over other particulate control devices: low operating cost, high collection performance, and easy maintenance.

Experiments have been carried out as a function of the switching frequency and duty ratio to investigate the smoke removal characteristics of the ESP.

2. The principle of dust collecting

When the high voltage is switched on the discharge electrode, the surface charge density on the side of the discharge electrode is greater than that of the opposite side. Therefore, a greater electrostatic force will pull the discharge electrode towards the collecting electrode in the opposite direction. This asymmetry of the surface charge density produces a negative resultant force upon the

discharge electrode, oriented towards the collecting electrode. At the same time a similarly asymmetrical charge distribution on the collecting electrode creates a positive force pulling the rounded edge of the collecting electrode towards the discharge electrode. These two forces cancel each other out. However, this situation is only a transient phase and its duration is very short.

Due to the presence of cosmic rays, there are always a minor quantity of ions and free electrons in the atmosphere. In the presence of an electric field, these free charges start to move in the direction of the E-field, and represent non-self-sustaining conduction. When the E-field intensity near the discharged electrode's surface rises above the break-down strength of the air, the ionization process starts. In such a strong E-field a free electron will be accelerated between two collisions, and it will gain enough kinetic energy to tear off one more electron from a neutral air molecule during the collision. Thus, a self-sustaining ionization process starts (self-conduction) because an additional free electron and positive ion have been created. These two free electrons will now create two more free electrons and positive ions, and this chain reaction will transform the air within the corona region (that was originally a good insulator) into conductive plasma. The free electrons will quickly move towards the collecting electrode, while the positive ions slowly move away from the discharged electrode, since their mass is much greater than that of the electrons. When the positive ions travel away from the surface of the discharged electrode, neutral air molecules move into their place sucked in by a pressure drop, while not being repelled by the intense E-field (unlike the + ions). Actually the neutral molecules will be polarized by the strong E-field and they will be attracted towards the regions of greater E-field intensity.

Directly above the surface of the discharge electrode a thin layer of negative space charge will develop, consisting of the rapidly approaching electrons (which finally enter into the discharge electrode); then outside a quasi-neutral region a dense positive space charge cloud will surround the discharge electrode. These positive ions are accelerating in the direction of the E-field lines and as a result, encounter many collisions with neutral air molecules before reaching the negative plate. In so doing, they give their momentum over to the neutral mass of air. This represents the ion drift process [4].

3. Design

Fig. 1 shows a schematic diagram for experimental setup composed of control part, electrode, power supply, and measuring instrument.

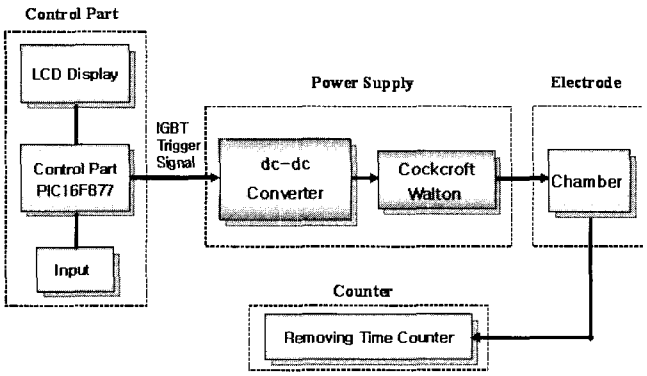

Fig. 1 Schematic diagram for experimental setup

3.1 Control circuit

The control circuit consists of a keyboard, LCD (liquid crystal display), PIC one-chip microprocessor (16F877) and the driving circuit to turn on the IGBT (Insulated gate bipolar transistor). In this control circuit, switching frequency and duty ratio are entered by keyboard, and this input information is transferred to the PIC. The PIC generates signals for driving the IGBT.

Fig. 2 displays an IGBT driving signal at the condition of duty ratio 50% as switching frequency 3 kHz and 9 kHz.

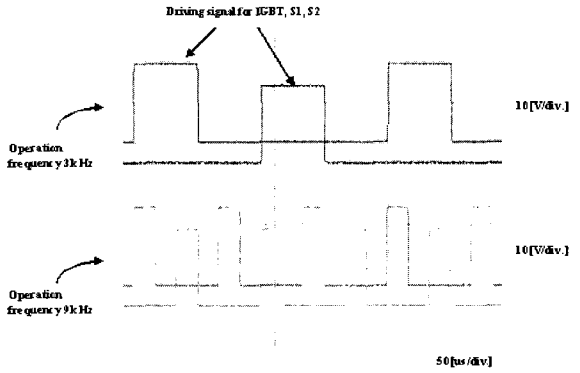

Fig. 2 IGBT driving signal versus switching frequency

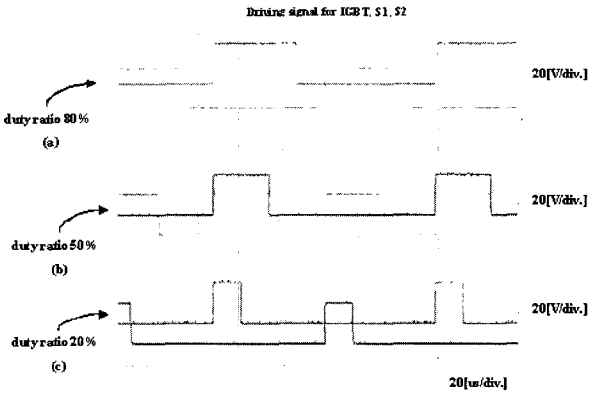

Fig. 3 IGBT driving signal versus duty ratio

Fig. 3 indicates an IGBT driving signal at the condition of a switching frequency 9 kHz with duty ratio at 20%, 50% and 80%.

3.2 High voltage power supply

Fig. 4 shows a power supply with high voltage dc-dc converter. Our power supply was designed and fabricated to pursue the high frequency range and to reduce switching loss and noises.

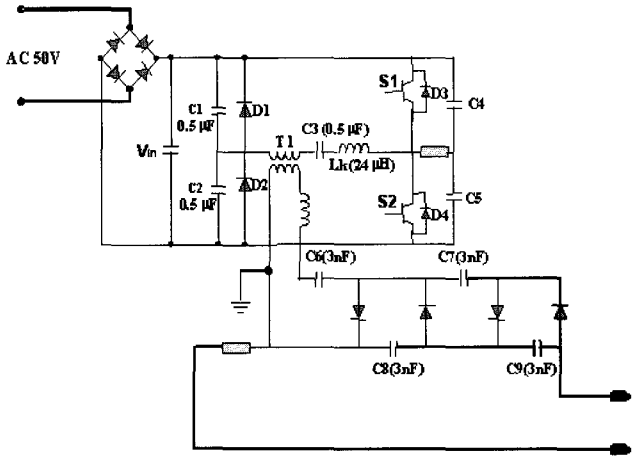

Fig. 4 Power supply with high voltage dc-dc converter

The circuit consists of a high power resonant inverter in half-bridge configuration, a high frequency step-up transformer and a high voltage rectifier using a Cockroft-Walton voltage multiplier.

The high voltage asymmetrical cascade rectifier was made to our specifications. The high voltage supply includes a 2 stage voltage multiplier driven by a regulated half-bridge inverter operating below resonance. The inverter drives the step up transformer and the transformer secondary is applied to a voltage multiplier. This combination guarantees small parasitic capacitance in the transformer stage, and speedy dynamic response. In particular, the ZCS series resonant inverter was used to decrease the losses by the tailing current generated upon turning off of the IGBT (Insulated gate bipolar transistor) [5].

3.2.1 Resonant inverter

The ZCS series resonant inverter consists of two IGBTs (S1, S2), a leakage inductor (L), blocking capacitor (C3), and charging capacitors (C1, C2). The switching loss is zero in principle, which is adequate during high repetition rate operation because the current through S1, S2, C1, and C2 is forced to the sinusoidal wave, and the switch devices are turned on/off at zero current. The output of the ZCS series resonant inverter is

$$P_{out} = 2fCV_{in}^2$$

Where f is the operating frequency, C is the capacitance of the charging capacitor, and V is the input voltage. According to this formula, it is found that there are two ways to control the power density of the resonant inverter. One is to vary the input voltage Vin at a constant pulse width and frequency, and the other is to adjust the switching frequency f.

The proposed ZCS inverter equivalent circuit and operating modes are shown in Fig. 5. The switching IGBT S1 and S2 form only one side of the bridge-connected circuit, the remaining half being formed by the C1 and C2 capacitors.

The diodes (D3, D4) that are connected in anti-parallel to the IGBTs are called freewheeling diodes. These diodes are able to provide a path for the resonant current in the direction opposite to the current direction in the IGBTs when the corresponding switch around which it is connected is in the off position. This is particularly important because the load is reactive.

Components C4, C5 and R1 are often referred to as snubber components; they assist the turn-off action of the high-voltage IGBT S1 and S2 so as to reduce secondary breakdown stress. As the IGBTs turn off, the transformer inductance maintains current flow, and the snubber components provide an alternative path for this current, preventing excessive voltage stress during the turn-off action.

The inverter switches may be in one of three different configurations at any given time; 1) S1 may be closed (on) while S2 is open (off), 2) S1 may be open while S2 is closed, or 3) both switches may be open.

Since C1 and C2 are the charging capacitors, they have a small capacitance. Before the power supply operates, capacitors C1 and C2 are initially equally charged so that the voltage at the center point, node A, will be half the supply voltage V. However, under steady-state conditions, the voltage at the center point of C1 and C2 will change significantly during an operating cycle even though the value of the voltage sum of the two capacitors is equal to that of input voltage Vin.

The circuit operation can be divided into three modes under steady state.

Mode 1(t0 ≤ t < t1): The equivalent circuits are shown in Fig. 5(a). When the top IGBT S1 turns on at time t0, a voltage of C1 will be applied across the primary winding of the step-up transformer T1 with the start going positive. The resonant current I_T flows through the path C1→S1→C3→Llk→T1→C1 and the path Vin→S1→C3→Llk→T1→C2. This process charges C2 during C1 discharge to the load. As a result of that, the value of the

charging capacitor voltage VC1 becomes zero with discharging and that of VC2 becomes that of input voltage Vin with charging as can be seen in Fig. 7.

Mode 2(t1 ≤ t < t2): The current through a leakage inductor Llk begins to flow through C3→Llk→T1→D1→S1→C3 at t1 as can be seen in Fig. 5(b). A reflected load current and magnetization current will now build up in the transformer primary and S1. After the time defined by the control circuit, S1 will be turned off at t2.

Mode 3(t2 ≤ t < t3): The equivalent circuit is presented in Fig. 5(c). Even though the IGBT S1 is turned off at time t2, as a result of the primary leakage inductance, resonant current will continue to flow into the start of the primary winding through C3→Llk→T1→D1→Vin→D4→C3. If the energy stored in the primary leakage inductance is sufficiently large, diode D4 will be brought into conduction to clamp any further negative excursion and return the remaining fly back energy to the supply.

After a period defined by the control circuit, S2 will also turn on, taking the start of the primary winding negative. Load and magnetizing currents will now flow in S2 and into the transformer primary winding finish so that the former process will repeat, but with primary current in the opposite direction. The difference is that at the end of an "on" period D3 is brought into conduction, returning the leakage inductance energy to the supply line (Vin). The value of VC1 becomes that of Vin and that of VC2 will be zero with being discharged to load after S2 turns off. Fig. 6 shows the voltages of the charging capacitors (C1, C2), resonant current (I_T), and current through diode (D1) during a switching cycle (S1: turn on, S2: turn off).

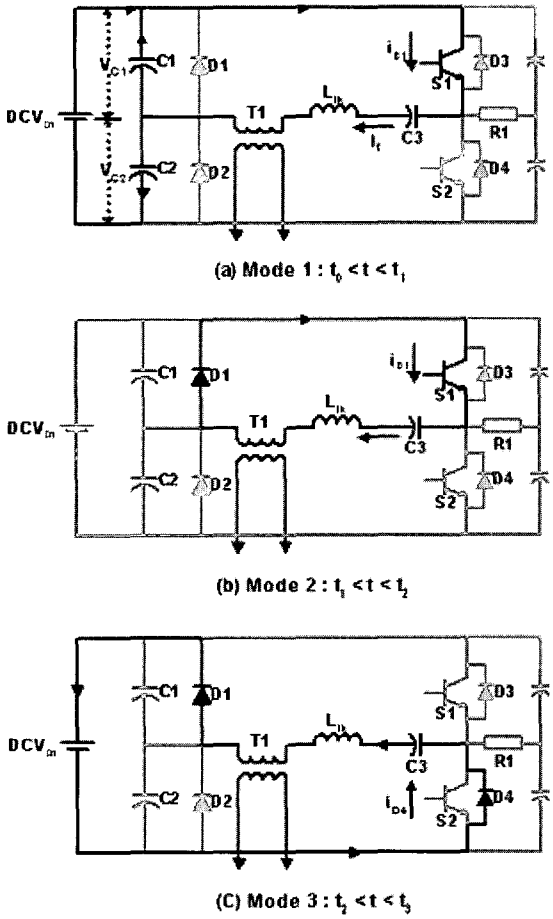

Fig. 5 Equivalent circuit of operation modes for the ZCS resonant inverter divided into three modes

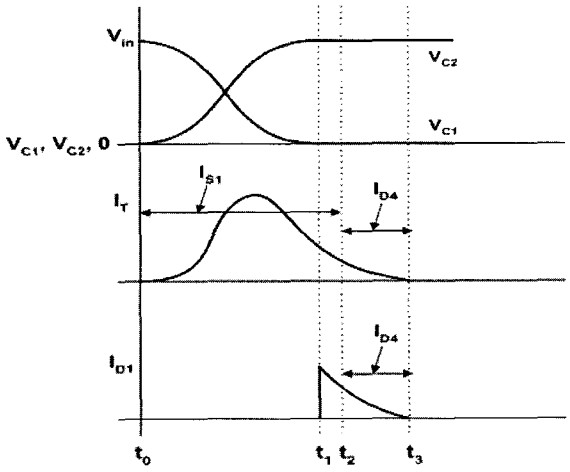

Fig. 6 Voltage of charging capacitors (C1, C2), resonant current (I_T), and current through diode (D1) during a switching cycle

3.2.2 The transformer

The transformer used in this circuit was wound on a fly back ferrite core (FUR5177S) constructed by Samhwa Electronics Inc., Korea. The secondary was wound on top of the primary with a layer of teflon tape between the two windings for insulation. Litz wire was used for firm coupling and the primary was rounded to the nearest lower turn. The primary voltage of the transformer was calculated considering voltage drops. The secondary transformer voltage can be derived considering diode drops, and other loss factors. As a result, the turn ratio of the transformer was determined to be 1:17. The primary winding turns was 40 turns and the secondary winding turns was 700 turns.

3.2.3 Cockcroft-Walton Voltage Multiplier

A 2 stage Cockcroft-Walton voltage multiplier serves as a high voltage generator to carry out the glow discharge in this ESP. A simplified analysis of the cascade rectifier operation, constructed in an asymmetrical fashion, shows that energy is transferred from the source (step-up transformer) to C6 (Fig. 4), which transfers it to C8 and so forth. An n-stage cascade rectifier can provide a dc output voltage of magnitude 2n V_p under no-load conditions (V_p is the peak value of the ac power source). The ESP can be considered as a resistive load during a corona-discharge process. Thus, the average output voltage will be smaller

than the value 2n V_p due to a load current dependent voltage drop. A 2-stage cascade rectifier, in this circuit, can provide a dc output voltage of more than 4kV under no load condition and an input voltage of AC 50V because the peak voltage value from step-up pulse transformer is about 1.1kV. In the Cockcroft-Walton circuit, the capacitance of C6~C9 is 3nF and the diodes are RVT1500 (fast recovery diodes).

3.3 Electrodes

Fig. 7 illustrates a chamber of our ESP with discharge electrode and collecting electrode. The type of electrode that is sealed using a double layered plate-plate device is made of stainless steel. The electrode is punched in the shape of a triangle that is able to form a uniform electric field. The construction of double layers is more efficient in the collection of smoke and dust. The size of the electrode is 140mm x 110mm. The thickness is 1.2mm.

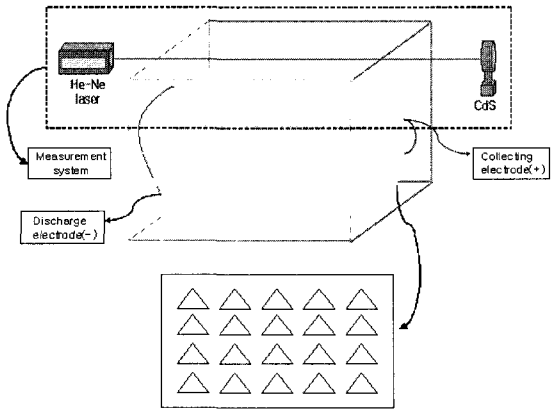

Fig. 7 Chamber of our ESP with discharge electrode and collecting electrode

3.4 Measuring instrument system

Fig. 7 also shows a measuring instrument system to count the smoke removal time of our ESP. We have carried out the smoke removal experiment as the function of the elapsed time from the initial voltage.

Fig. 8 shows the test equipment circuit.

We are able to monitor the degree of turbidity through the change of the broad light intensity of the He-Ne laser, which depends on turbidity in the chamber. When the degree of turbidity in the experimental chamber is changed, the CdS sensor is able to detect the change of the He-Ne laser broad light intensity. We used a comparison circuit to precisely count the smoke removal time. The voltage change signal due to the resistance change of the CdS sensor is connected directly to the op-amp's non-inverting terminal (1) in Fig. 8. On the other hand, the inverting terminal (2) in Fig. 8 is connected to the voltage set by the voltage divider. Because the voltage signal from the CdS is proportional to the broad light intensity, if the input signal becomes more positive than the reference voltage, which is 8V in this system, the output signal from the op-amp become high. As soon as the input signal goes below 8V, the output signal from the transistor is changed to low. Using this measurement system, we can calculate the smoke removal time.

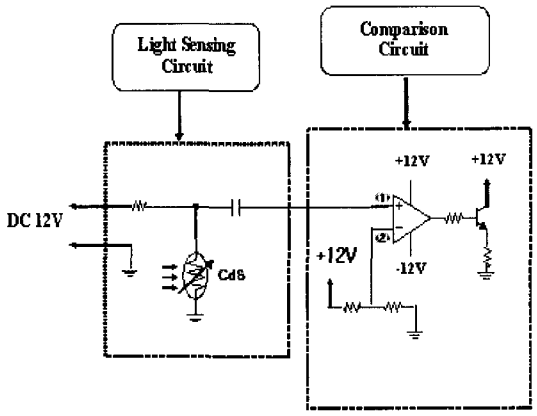

Fig. 8 Test equipment circuit

4. Result and Discussion

The purpose of this study is to investigate the smoke removal characteristics of a ZCS dc-dc converter using a Cockroft-Walton circuit, which has been manufactured and tested in a laboratory. Accordingly, we introduce dirty gas containing particulate pollutants into the test chamber and investigate the smoke removal characteristics by adjusting the frequency and duty ratios from an identical test environment. Furthermore, we have carried out the smoke removing experiment as a function of the elapsed time from the initial voltage.

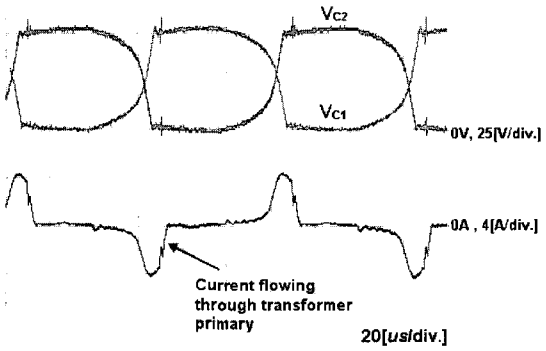

Fig. 9 Current waveform flowing through the transformer primary and voltage of the resonant capacitor V_{C1} and V_{C2}

Fig. 9 shows the current flowing through the primary of the transformer and the voltage of the charging capacitor.

Fig. 10 depicts the experimental waveform for the collector-to-emitter voltage, current of the IGBT S1 and the bypass current flowing through the freewheeling diode D3 when S2 is turned off.

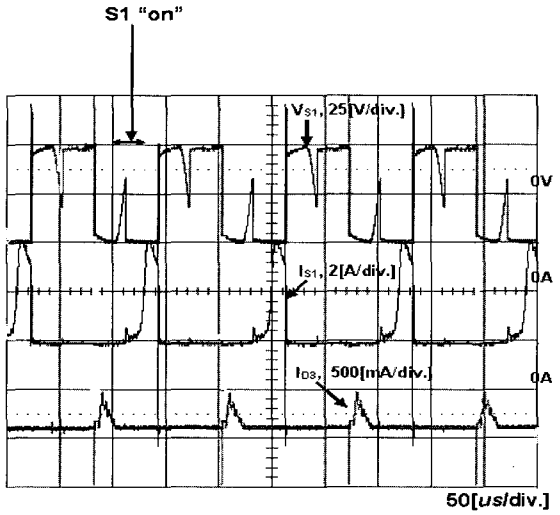

Fig. 10 Experimental waveforms for collector-to-emitter voltage and S1 current and bypass current flowing through diode D3

Fig. 11 illustrates a voltage waveform from the driving circuit used in turning on the IGBTs and the current waveform flowing through the primary of the transformer. The current waveform is similar to a sinusoidal wave and both can demonstrate ZCS operation. Thanks to this ZCS operation, switching losses are considerably relieved. The switching stress is also essential from the viewpoint of conducted EMI (electromagnetic interference), but the application of the soft-switching technique can not only reduce switching losses but also lower the conducted EMI levels [6].

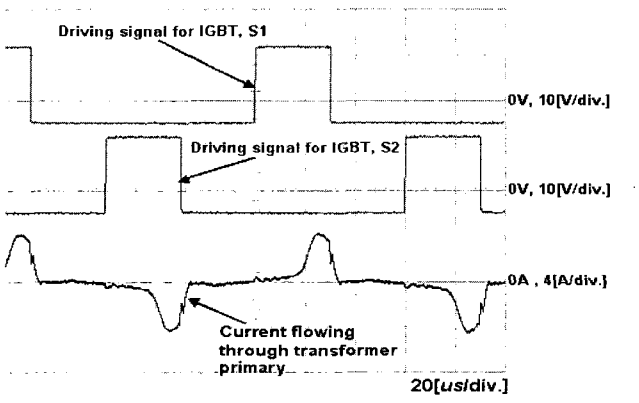

Fig. 11 IGBT driving signals and current waveform flowing through the transformer primary

In this study, if the initial applied voltage is much higher than 50V, the smoke removal time is too short and we cannot calculate it. Therefore, we fixed the applied initial voltage at 50V.

Fig. 12 shows the smoke removal time by adjusting the switching frequency. The smoke removal time is decreased according to increase in the switching frequency. The lowest smoke removal time is 2.56s at switching frequency condition of 9 kHz and all duty ratios.

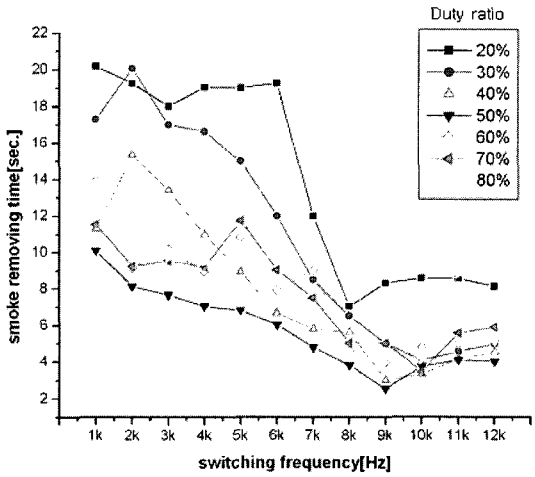

Fig. 12 The smoke removing time versus switching frequency

Fig. 13 depicts the smoke removal time by adjusting duty ratio at 9 kHz. The longest smoke removal time is 2.56s at the 50% duty ratio, because the maximum energy is delivered to the system, at this duty ratio.

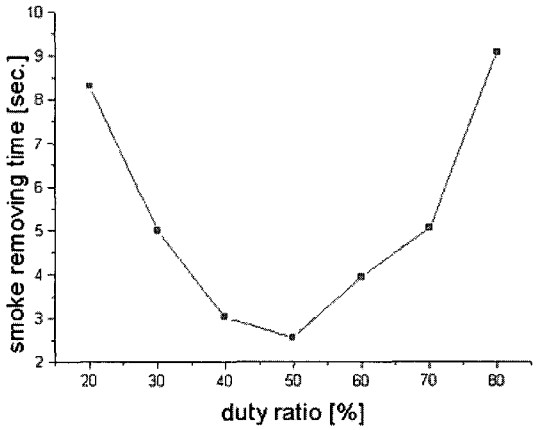

Fig. 13 Smoke removal time versus duty ratio

Fig. 14 shows the inverter input current by varying switching frequency at a fixed input voltage of 50 V. As a result, the highest current of 186mA was obtained at the switching frequency of 9 kHz. The inverter input current increases according to increase in the frequency. The corona discharge current increases with total input power.

As the corona discharge current rises, the number of free electrons increases, which leads to an enforced electronic excitation of the dirty gas. If input power is greater than a certain saturation value, corona discharge becomes unstable and collapses into arc-like filaments or streamers. This circuit operates under resonance conditions with the result being that the rising rate of total switching loss is low even though the operating frequency increases. However, inverter input current is decreased at 10 kHz, because this frequency, 9 kHz, is nearly identical to the resonant frequency in the circuit.

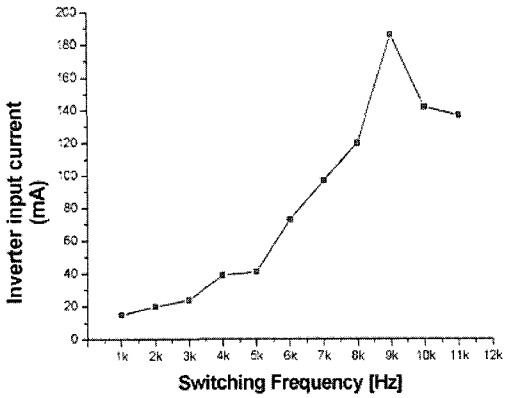

Fig. 14 Inverter input current versus switching frequency

5. Conclusion

In this study, we proposed an electrostatic precipitator (ESP) adopted dc-dc converter system with the current resonant half-bridge inverter and the Cockcroft-Walton circuit.

We investigated the smoke removal characteristics of this ESP as a function of a switching frequency and a duty ratio. We found the best switching frequency and duty ratio in our system. The obtained results are as follows.

1. As the switching frequency changes from 2 to 12 kHz, the least smoke removal time is obtained at the switching frequency of 9 kHz at the condition of all the duty ratios and the applied voltage of 3.4 kV.

2. As the duty ratio changes from 20 to 80% at the condition of switching frequency (9 kHz), the least smoke removal time obtained is 2.56s at the duty ratio of 50% and the applied voltage of 3.4 kV.

3. From these experimental results, the best operational condition is obtained at the switching frequency of 9 kHz and the duty ratio of 50 % in this ESP.

References

[1] S. Cristina and M. Feliziani, Industry Applications Society Annual Meeting, 1991.; Conference Record of the 1991 IEEE , 28 Sept.-4 Oct. 1991 pp. 616 -621 vol.1

[2] A. Zukeran, P.C. Looy, A. Chakrabarti, A.A. Berezin, S. Jayaram, J.D. Cross, T. Ito and Jen-Shih Chang; Industry Applications, IEEE Transactions on , Volume: 35 Issue: 5, Sept.-Oct. 1999 pp. 1184-1191

[3] A. Mizuno, Dielectrics and Electrical Insulation, IEEE Transactions on [see also Electrical Insulation, IEEE Transactions on] , Volume: 7Issue: 5, Oct. 2000 pp: 615-624

[4] D. Brocilo, J.S. Chang, R.D. Findlay, Y. Kawada and T. Ito, Electrical Insulation and Dielectric Phenomena, 2001 Annual Report. Conference on , 14-17 Oct. 2001 pp. 681 -684

[5] Y. Kotov, G. Mesyats, S. Rufkin, A. Filatov, and S. Lyubutin, "A novel nanosecond semiconductor opening switch for megavolt repetitive pulsed power technology: Experiment and application," in Proc IX Int. IEEE Pulsed Power Conf., Albuquerque. NM, 1993. pp. 134-139

[6] R.L. Steigerwald, Industrial Electronics, Control, and Instrumentation, 1995., Proceedings of the 1995 IEEE IECON 21st International Conference on , Volume: 1 , 6-10 Nov. 1995 pp. 1 -7 vol.1

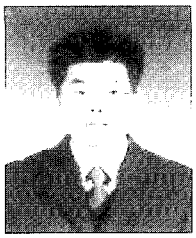

Su-Weon Kim

He received his B.S. degree in Electrical Engineering from Pusan National University in 2002. He received his M.S. degree in Electrical Engineering from Pusan National University in 2004

Jong -Woong Park

He received his B.S. degree in Electrical Engineering from Pukyong National University in 2003. Currently, he is working towards a M.S. degree in Electrical Engineering at Pusan National University.

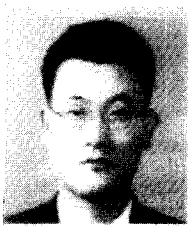

Jong-Han Jung
He received his B.S. degree in Electrical Engineering from Pusan National University of Technology in 1996. He received his M.S. and Ph.D. degrees in Electrical Engineering from Pusan National University in 1998 and 2003, respectively. He is currently a Research Professor of Electronic Communication Engineering at Chang-won College.

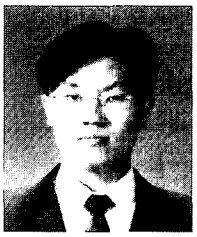

Hyun-Ju Chung
He received his M.S. degree in Electrical Engineering from Pusan National University, Korea in 2000. Currently, he is working toward his Ph.D. degree in Electrical Engineering at Pusan National University. He has been working in the Agency for Defense Development, Korea, since 2002.

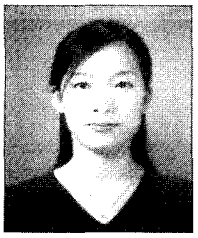

Jin-Young Choi
She received her B.S. degree in Optics Engineering from Silla University in 2002. Currently, she is working towards a M.S. degree in Electrical Engineering at Pusan National University.

Hee-je Kim
He received his B.S. and M.S. degrees in Electrical Engineering from Pusan National University, Korea in 1980 and 1982, respectively. He joined the Plasma & Laser Lab of the Korea Electro-Technology Institute in 1983 as a Research Engineer and went to Kyushu University, Hukuoka, Japan in 1985 where he received his Ph.D. degree in 1990. From 1995 to the present he has been a Professor at the School of Electrical Engineering, Pusan National University.